SPACE MAPPING OPTIMIZATION FOR ENGINEERING DESIGN

JOHN W. BANDLER[*+], RADEK M. BIERNACKI[*+], SHAOHUA CHEN[*+], RONALD H. HEMMERS[+] AND KAJ MADSEN[†]

Abstract. This contribution describes the Space Mapping (SM) technique which is relevant to engineering optimization. The SM technique utilizes different models of the same physical object. Similarly to approximation, interpolation, variable-complexity, response surface modeling, surrogate models, and related techniques, the idea is to replace computationally intensive simulations of an accurate model by faster though less accurate evaluations of another model. In contrast, SM attempts to establish a mapping between the input parameter spaces of those models. This mapping allows us to redirect the optimization-related calculations to the fast model while preserving the accuracy and confidence offered by a few well-targeted evaluations of the accurate model. The SM technique has been successfully applied in the area of microwave circuit design. In principle, however, it is applicable to a wide range of problems where models of different complexity and computational intensity are available, although insight into engineering modeling in the specific application area might be essential.

Key words. Space Mapping, Design Optimization, Engineering Modeling.

1. Introduction. Advances in computing technology provide engineering designers with more and more sophisticated simulation tools that can more and more accurately predict the behaviour of more and more complex objects. For design optimization, this means that the simulation times rather than the optimization algorithms become a true bottleneck and limiting factors for various applications. For such applications the scale of optimization is measured not in terms of the number of variables, but rather in terms of real time needed to complete it. A small electronic circuit may require weeks of simulation time and only a small fraction of a second for the optimizer to determine the next point.

This paper describes the concept of Space Mapping (SM) [2-8]. The SM technique exploits a mathematical link between input parameters of different engineering models of the same physical object: (1) a computationally efficient (fast) model which may lack the desired accuracy, and (2) an

---

[*] Optimization Systems Associates Inc., P.O. Box 8083, Dundas, Ontario, Canada L9H 5E7. The work of the first three authors was supported in part by Optimization Systems Associates Inc.

[+] The Simulation Optimization Systems Research Laboratory and Department of Electrical and Computer Engineering, McMaster University, Hamilton, Ontario, Canada L8S 4L7. The work of the first four authors was supported in part by the Natural Sciences and Engineering Research Council of Canada under Grants OGP0007239, OGP0042444, STR0167080 and through the Micronet Network of Centres of Excellence.

[†] Institute of Mathematical Modeling, Technical University of Denmark, DK-2800 Lyngby, Denmark.

accurate but CPU-intensive model. Traditionally, there exists a number of engineering models of different types and levels of complexity to choose from. In the field of electronic circuits this may include equivalent circuit models, ideal and detailed empirical models, electromagnetic (EM) field theory based models, hybrid models [20], and even computational utilization of actual hardware measurements.

As a fast model we want to use an engineering model that is capable of reasonably emulating the behaviour of the actual physical object, for example of generating a band-selective response of a filter. Such a model may be an otherwise good empirical model, however, the parameter values might be outside their recommended validity ranges. It may also be the same simulator which is used as the accurate model, e.g., an electromagnetic field solver, but with a coarser grid size than required to produce accurate results [4,5].

Similarly to various approximation and interpolation [10,11], variable-complexity [13,15,16], response surface modeling [19], surrogate models [23], and related techniques [21,22], the idea of SM is to replace computationally intensive simulations of an accurate model by faster though less accurate evaluations of another model. In contrast to those methods, SM attempts to establish a mapping between the input parameter spaces of those models, instead of trying to refine and validate the fast model using the same parameter values as for the accurate model. The underlying assumption is that the inaccuracy of the fast model can be somehow compensated for by adjusting the model parameter values.

The SM concept facilitates the demanding requirements of otherwise CPU-prohibitive design optimization within a practical time frame. This is accomplished by redirecting the optimization-related calculations to the fast model while preserving the accuracy and confidence offered by a few well-targeted evaluations of the slow accurate model.

There are two phases in SM. In *Phase* 1, optimization is performed using the fast model to obtain its optimal performance. In *Phase* 2, a mapping between the input parameter spaces of the two models considered is iteratively established. Techniques such as least-squares or quasi-Newton steps are used to accomplish this. A distinct auxiliary optimization (parameter extraction), also using the fast model, must be invoked in each iteration of *Phase* 2. This parameter extraction is used to determine the parameters of the fast model such that its response(s) match those of the reference response(s) obtained from an evaluation of the accurate model. The uniqueness of the parameter extraction process is of utmost importance to the success of SM.

The SM technique has been successfully applied in the area of microwave circuit design. In principle, however, it is applicable to a wide variety of problems where models of different complexity and computational intensity are available, although insight into engineering modeling in the specific application area might be essential.

Our presentation describes the theoretical formulation of SM followed by a practical

engineering example: design of a high-temperature superconducting (HTS) microstrip filter. In this particular case we consider an equivalent empirical circuit model as the fast model. As the accurate model, we employ an extremely CPU-intensive model based on solving electromagnetic field equations.

2. Space Mapping Optimization.

2.1. Theory. Let the behaviour of a system be described by models in two spaces: the optimization space, denoted by X_{os}, and the EM (or validation) space, denoted by X_{em}. We represent the optimizable model parameters in these spaces by the vectors x_{os} and x_{em}, respectively. We assume that X_{os} and X_{em} have the same dimensionality, i.e., $x_{os} \in \mathbb{R}^n$ and $x_{em} \in \mathbb{R}^n$, but may not represent the same parameters. We assume that the X_{os}-space model responses, denoted by $R_{os}(x_{os})$, are much faster to calculate but less accurate than the X_{em}-space model responses, denoted by $R_{em}(x_{em})$.

The key idea behind SM optimization is the generation of an appropriate mapping, P, from the X_{em}-space to the X_{os}-space,

$$x_{os} = P(x_{em}) \tag{2.1}$$

such that

$$R_{os}(P(x_{em})) \approx R_{em}(x_{em}). \tag{2.2}$$

We assume that such a mapping exists and is one-to-one within some local modeling region encompassing our SM solution. We also assume that, based on (2.2), for a given x_{em} its image x_{os} in (2.1) can be found by a suitable parameter extraction procedure, and that this process is unique.

We initially perform optimization entirely in X_{os} to obtain the optimal solution x_{os}^*, for instance in the minimax sense [9], and subsequently use SM to find the mapped solution $\bar{x}_{em}$ in X_{em} as

$$\bar{x}_{em} = P^{-1}(x_{os}^*) \tag{2.3}$$

once the mapping (2.1) is established. We designate $\bar{x}_{em}$ as the SM solution instead of x_{em}^* since the mapped solution represents only an approximation to the true optimum in X_{em}.

The mapping is established through an iterative process. We begin with a set of m X_{em}-space model base points

(2.4) $$B_{em} = \{ x_{em}^{(1)},\ x_{em}^{(2)},\ \ldots,\ x_{em}^{(m)} \}.$$

These initial m base points are selected in the vicinity of a reasonable candidate for the X_{em}-space model solution. For example, if x_{em} and x_{os} consist of the same physical parameters, then the set B_{em} can be chosen as

(2.5) $$x_{em}^{(1)} = x_{os}^{*}$$

with the remaining $m-1$ base points chosen arbitrarily by perturbation as

(2.6) $$x_{em}^{(i)} = x_{em}^{(1)} + \Delta x_{em}^{(i-1)}, \quad i = 2, 3, \ldots, m.$$

For instance, for a linear mapping, one can select perturbations along the axes. Once the set B_{em} is chosen, we perform EM analyses at each base point to obtain the X_{em}-space model responses $R_{em}(x_{em}^{(i)})$ for $i = 1, 2, \ldots, m$. This is followed by parameter extraction optimization in X_{os} to obtain the corresponding set of m X_{os}-space model base points

(2.7) $$B_{os} = \{ x_{os}^{(1)},\ x_{os}^{(2)},\ \ldots,\ x_{os}^{(m)} \}.$$

The parameter extraction process is carried out by the following optimization:

(2.8) $$\underset{x_{os}^{(i)}}{\text{minimize}} \ \| R_{os}(x_{os}^{(i)}) - R_{em}(x_{em}^{(i)}) \|$$

for $i = 1, 2, \ldots, m$ where $\|\cdot\|$ indicates a suitable norm. The additional $m-1$ points apart from $x_{em}^{(1)}$ are required merely to establish full-rank conditions leading to the initial approximation of the mapping (denoted by P_0 - its exact construction is explained later).

At the jth iteration, both sets may be expanded to contain, in general, m_j points which are used to establish the updated mapping P_j. Since the analytical form of P is not available, we use the current approximation P_j to estimate $\bar{x}_{em}$ in (2.3), i.e.,

(2.9) $$x_{em}^{(m_j+1)} = P_j^{-1}(x_{os}^{*}).$$

The process continues iteratively until the termination condition

$$\| R_{os}(x_{os}^{*}) - R_{em}(x_{em}^{(m_j+1)}) \| \leq \epsilon \tag{2.10}$$

is satisfied, where ϵ is acceptably small. If so, P_j is our desired P. If not, the set of base points in B_{em} is augmented by $x_{em}^{(m_j+1)}$ and correspondingly, $x_{os}^{(m_j+1)}$ determined by (2.8) augments the set of base points in B_{os}. Upon termination, we set $\bar{x}_{em} = x_{em}^{(m_j+1)} = P_j^{-1}(x_{os}^{*})$ as the SM solution. This process is illustrated graphically in Fig. 1

We define each of the transformations P_j as a linear combination of some predefined and fixed fundamental functions

$$\hat{f}_1(x_{em}),\ \hat{f}_2(x_{em}),\ \hat{f}_3(x_{em}),\ \ldots,\ \hat{f}_t(x_{em}) \tag{2.11}$$

such that

$$x_{os_i} = \sum_{s=1}^{t} a_{is} \hat{f}_s(x_{em}) \tag{2.12}$$

or, in matrix form

$$x_{os} = P_j(x_{em}) = A_j \hat{f}(x_{em}) \tag{2.13}$$

where A_j is an $n \times t$ matrix, $\hat{f}(x_{em})$ is a t-dimensional column vector of fundamental functions.

Consider the mapping P_j for all points in the sets B_{em} and B_{os}. Expanding (2.13) gives

$$\left[x_{os}^{(1)}\ x_{os}^{(2)}\ \ldots\ x_{os}^{(m_j)} \right] = A_j \left[\hat{f}(x_{em}^{(1)})\ \hat{f}(x_{em}^{(2)})\ \ldots\ \hat{f}(x_{em}^{(m_j)}) \right] \tag{2.14}$$

where $m_j \geq t$.

The simplest choice, frequently adequate for local problems, is to consider a linear mapping. In this particular case, $\hat{f}(x_{em})$ in (2.11) contains the $n+1$ linear functions: 1, x_{em_1}, x_{em_2}, ..., x_{em_n}. Hence, (2.14) can be written as

$$\left[x_{os}^{(1)} \;\; x_{os}^{(2)} \;\; \ldots \;\; x_{os}^{(m_j)} \right] = Q_j \left[x_{em}^{(1)} \;\; x_{em}^{(2)} \;\; \ldots \;\; x_{em}^{(m_j)} \right] + \left[b_j \;\; b_j \;\; \ldots \;\; b_j \right]$$

(2.15)

$$= \left[b_j \; Q_j \right] \begin{bmatrix} 1 & 1 & \ldots & 1 \\ x_{em}^{(1)} & x_{em}^{(2)} & \ldots & x_{em}^{(m_j)} \end{bmatrix}$$

where Q_j is an $n \times n$ matrix and b_j is an $n \times 1$ column vector. Let us define

(2.16) $$C = \left[x_{os}^{(1)} \;\; x_{os}^{(2)} \;\; \ldots \;\; x_{os}^{(m_j)} \right]^T,$$

(2.17) $$D = \left[\hat{f}(x_{em}^{(1)}) \;\; \hat{f}(x_{em}^{(2)}) \;\; \ldots \;\; \hat{f}(x_{em}^{(m_j)}) \right]^T = \begin{bmatrix} 1 & 1 & \ldots & 1 \\ x_{em}^{(1)} & x_{em}^{(2)} & \ldots & x_{em}^{(m_j)} \end{bmatrix}^T$$

and

(2.18) $$A_j = \left[b_j \; Q_j \right].$$

Then (2.14) becomes

(2.19) $$C^T = A_j D^T.$$

Transposing both sides of (2.19) gives

(2.20) $$D A_j^T = C.$$

Augmenting (2.20) by some weighting factors defined by an $m_j \times m_j$ diagonal matrix W, where

(2.21) $$W = diag\{w_i\}$$

gives

(2.22) $$\boldsymbol{W}\boldsymbol{D}\boldsymbol{A}_j^T = \boldsymbol{W}\boldsymbol{C}.$$

The least-squares solution to this system is

(2.23) $$\boldsymbol{A}_j^T = \left(\boldsymbol{D}^T\boldsymbol{W}^T\boldsymbol{W}\boldsymbol{D}\right)^{-1}\boldsymbol{D}^T\boldsymbol{W}^T\boldsymbol{W}\boldsymbol{C}.$$

Larger/smaller weighting factors emphasize/deemphasize the influence of the corresponding base points on the SM transformation.

2.2. Implementation. We now present a straightforward implementation of the SM algorithm. First, begin with a point, $\boldsymbol{x}_{os}^* \triangleq arg\ min\{H(\boldsymbol{x}_{os})\}$, representing the optimal solution in $\boldsymbol{X}_{os}$ where $H(\boldsymbol{x}_{os})$ is some appropriate objective function. Then, the algorithm proceeds as follows:

Step 0. Initialize $\boldsymbol{x}_{em}^{(1)} = \boldsymbol{x}_{os}^*$. If $\| \boldsymbol{R}_{os}(\boldsymbol{x}_{os}^*) - \boldsymbol{R}_{em}(\boldsymbol{x}_{em}^{(1)}) \| \le \epsilon$, stop. Otherwise, initialize $\Delta\boldsymbol{x}_{em}^{(i-1)}$ for $i = 2, 3, ..., m$.

Step 1. Select $m-1$ additional base points in $\boldsymbol{X}_{em}$ by perturbation, i.e., $\boldsymbol{x}_{em}^{(i)} = \boldsymbol{x}_{em}^{(1)} + \Delta\boldsymbol{x}_{em}^{(i-1)}$ for $i = 2, 3, ..., m$.

Step 2. Perform parameter extraction optimization to obtain $\boldsymbol{x}_{os}^{(i)}$ for $i = 1, 2, ..., m$.

Step 3. Initialize $j = 0$, $m_j = m$.

Step 4. Compute $\boldsymbol{A}_j^T = \left(\boldsymbol{D}^T\boldsymbol{W}^T\boldsymbol{W}\boldsymbol{D}\right)^{-1}\boldsymbol{D}^T\boldsymbol{W}^T\boldsymbol{W}\boldsymbol{C}$ and extract the matrix $\boldsymbol{Q}_j$ and the vector $\boldsymbol{b}_j$ according to $\boldsymbol{A}_j = \left[\boldsymbol{b}_j \ \ \boldsymbol{Q}_j\right]$.

Step 5. Set $\boldsymbol{x}_{em}^{(m_j+1)} = \boldsymbol{Q}_j^{-1}(\boldsymbol{x}_{os}^* - \boldsymbol{b}_j)$.

Step 6. If $\| \boldsymbol{R}_{os}(\boldsymbol{x}_{os}^*) - \boldsymbol{R}_{em}(\boldsymbol{x}_{em}^{(m_j+1)}) \| \le \epsilon$, stop.

Step 7. Perform parameter extraction optimization to obtain $\boldsymbol{x}_{os}^{(m_j+1)}$.

Step 8. Augment the matrix $\boldsymbol{C}$ with $\boldsymbol{x}_{os}^{(m_j+1)}$ and the matrix $\boldsymbol{D}$ with $\boldsymbol{x}_{em}^{(m_j+1)}$.

Step 9. Set $j = j + 1$, $m_j = m_j + 1$; go to *Step* 4.

Comments

Note, that in *Steps* 2 and 7 an auxiliary optimization (parameter extraction) is invoked. In *Step* 5, $\boldsymbol{x}_{em}^{(m_j+1)}$ may be snapped to the closest grid point if the EM simulator uses a fixed-grid meshing scheme.

2.3. Aggressive Strategy for Space Mapping. An aggressive strategy has been derived for SM [7,8]. It exploits quasi-Newton iterations and Broyden update [12]. The aggressive approach is significantly more efficient than that described in the preceding subsection since it avoids performing time-consuming and possibly unproductive EM analyses at the perturbed points around the starting

point. Instead, right from the beginning, it attempts to improve the solution in a systematic manner by well-targeted and fewer EM simulations. Moreover, the aggressive approach is better suited for automation of the SM technique [2].

3. Design of a High-temperature Superconducting (HTS) Parallel Coupled-line Microstrip Filter Exploiting Space Mapping. The SM technique has been successfully applied to the design of an HTS filter. A detailed description of the filter (see Fig. 2) can be found in [3,6-8]. The filter uses microstrip technology where metallization strips are deposited on a solid dielectric substrate which separates the top metal strips and the bottom metal ground plane. Fig. 2 shows the top view of the metallization pattern. The dielectric and the ground plane box and their heights are not shown. The filter works as a two-port with the input and output ports located at the ends of leftmost and the rightmost strips. An electrical signal is transmitted from the input to the output by means of the electromagnetic field in the structure, including couplings between the strips. L_1, L_2 and L_3 are the lengths of the parallel coupled-line sections and S_1, S_2 and S_3 are the gaps between the sections. The width W is the same for all the sections as well as for the input and output microstrip lines, of length L_0. The thickness of the lanthanum aluminate substrate used is 20 mil. The dielectric constant and the loss tangent are assumed to be 23.425 and 3×10^{-5}, respectively. The metallization is considered lossless.

This relatively small circuit exemplifies difficulties in directly using detailed EM simulations during optimization. To obtain an accurate and detailed circuit response, such as the one drawn using the dashed line in Fig. 4, one needs more than a week of CPU time on a Sun SPARCstation 10. To invoke such simulations many times during optimization is prohibitive.

For this problem, we consider 6 optimization variables representing the geometrical dimensions of the filter: L_1, L_2, L_3, S_1, S_2 and S_3 . We employ two models: (1) a fast model, based on empirical formulas available in the OSA90/hope [18] software package, and (2) an accurate but extremely CPU-intensive model, based on solving electromagnetic field equations by the ***em*** simulator [14].

Following *Phase* 1 of SM, we optimize the HTS filter using the OSA90/hope empirical model. The optimization goal is formulated in terms of the so-called scattering parameters S. These S parameters quantify the filter behaviour in terms of the power transfer from the input to the output of the filter [17]. Of particular interest is the parameter $|S_{21}|$ and its dependence on frequency (frequency response). The filtering capabilities of the circuit considered are described by the design specifications:

$$|S_{21}| \le 0.05 \quad \text{in the stopband}$$
$$|S_{21}| \ge 0.95 \quad \text{in the passband}$$

where the stopband includes frequencies below 3.967 GHz and above 4.099 GHz and the passband lies

in the frequency range [4.008 GHz, 4.058 GHz]. An appropriate objective function for optimization is formulated from the design specifications [8]. Fig. 3 shows the $|S_{21}|$ (and $|S_{11}|$) empirical (fast) model responses after performing minimax optimization using OSA90/hope. Using the parameter values determined by minimax optimization the *em* simulated frequency response differs significantly from that of the empirical model, as shown in Fig. 4.

In *Phase* 2 of SM, our aim is to establish a mapping in order to find a solution in the EM space which substantially reproduces the performance predicted by the optimal empirical model. We report results obtained using the aggressive strategy (Section 2.3). The original approach (Sections 2.1 and 2.2) was also used and similar results were obtained. In this phase, in order to further reduce the CPU time of EM simulations, we do not consider as fine frequency sweeps as those shown in the figures. We use only 15 frequency points per sweep which turned out to be adequate. The SM solution emerges after only six such simplified EM analyses (13 for original SM). Fig. 5 compares the filter responses of the optimal empirical model and the *em* simulated SM solution.

4. Conclusions. This presentation has included a theoretical formulation of the Space Mapping technique and its application to the design of a high-temperature superconducting parallel coupled-line microstrip filter.

Space Mapping optimization is a newly emerging and very promising approach. It exploits the speed of an efficient surrogate model and blends it with a few slow evaluations of an accurate model to effectively perform design optimization within a practical time frame. A few recent publications in the engineering field exhibit some similarities to the concepts found in Space Mapping [13,15,16,21-23]. The main difference distinguishing Space Mapping from those techniques is that instead of trying to improve the surrogate models, it allows the input parameters of the fast model to be different from those in the actual physical object, or in the accurate model.

In the near future we expect to see the Space Mapping concept applied to active devices. In this domain, physics-based models and physical models will be utilized [1]. Physics-based models relate the equivalent circuit elements to the device physics based on simplified analytical solutions of device equations. Physical models, based on the numerical solution of fundamental device equations are the most accurate. However, they require significantly more computation time than the physics-based models. Hence, Space Mapping may be the key to achieving the accuracy of physical simulation and the speed of circuit-level optimization.

Surprisingly, the concept of Space Mapping is only now establishing itself in the domain of circuit optimization. This is despite the overwhelming array of engineering models of devices, circuits and systems. It should be noted that designers increasingly employ accurate CPU-intensive simulators, yet extensive use of efficient simplified models is made to avoid time-consuming analyses. SM bridges the two approaches and takes advantage of their respective benefits.

REFERENCES

[1] J.W. Bandler, "Statistical modeling, design centering, yield optimization and cost-driven design," *CAD Design Methodology for Commercial Applications*. Workshop WFFE (A.M. Pavio, Organizer and Chairman), IEEE MTT-S Int. Microwave Symp. (Orlando, FL), 1995.

[2] J.W. Bandler, R.M. Biernacki and S.H. Chen, "Fully automated space mapping optimization of 3D structures," *IEEE MTT-S Int. Microwave Symp.* (San Francisco, CA), June 1996.

[3] J.W. Bandler, R.M. Biernacki, S.H. Chen, W.J. Getsinger, P.A. Grobelny, C. Moskowitz and S.H. Talisa, "Electromagnetic design of high-temperature superconducting microwave filters," *Int. J. Microwave and Millimeter-Wave Computer-Aided Engineering*, vol. 5, 1995, pp. 331-343.

[4] J.W. Bandler, R.M. Biernacki, S.H. Chen, P.A. Grobelny and R.H. Hemmers, "Exploitation of coarse grid for electromagnetic optimization," *IEEE MTT-S Int. Microwave Symp. Dig.* (San Diego, CA), 1994, pp. 381-384.

[5] J.W. Bandler, R.M. Biernacki, S.H. Chen, P.A. Grobelny and R.H. Hemmers, "Space mapping technique for electromagnetic optimization," *IEEE Trans. Microwave Theory Tech.*, vol. 42, 1994, pp. 2536-2544.

[6] J.W. Bandler, R.M. Biernacki, S.H. Chen, P.A. Grobelny, C. Moskowitz and S.H. Talisa, "Electromagnetic design of high-temperature superconducting microwave filters," *IEEE MTT-S Int. Microwave Symp. Dig.* (San Diego, CA), 1994, pp. 993-996.

[7] J.W. Bandler, R.M. Biernacki, S.H. Chen, R.H. Hemmers and K. Madsen, "Aggressive space mapping for electromagnetic design," *IEEE MTT-S Int. Microwave Symp. Dig.* (Orlando, FL), 1995, pp. 1455-1458.

[8] J.W. Bandler, R.M. Biernacki, S.H. Chen, R.H. Hemmers and K. Madsen, "Electromagnetic optimization exploiting aggressive space mapping," *IEEE Trans. Microwave Theory Tech.*, vol. 43, 1995, pp. 2874-2882.

[9] J.W. Bandler and S.H. Chen, "Circuit optimization: the state of the art," *IEEE Trans. Microwave Theory Tech.*, vol. 36, 1988, pp. 424-443.

[10] R.M. Biernacki, J.W. Bandler, J. Song and Q.J. Zhang, "Efficient quadratic approximation for statistical design," *IEEE Trans. Circuits and Systems*, vol. 36, 1989, pp. 1449-1454.

[11] R.M. Biernacki and M.A. Styblinski, "Efficient performance function interpolation scheme and its application to statistical circuit design," *Int. J. Circuit Theory and Appl.*, vol. 19, 1991, pp. 403-422.

[12] C.G. Broyden, "A class of methods for solving nonlinear simultaneous equations," *Math. of Comp.*, vol. 19, 1965, pp. 577-593.

[13] S. Burgee, A.A. Guinta, R. Narducci, L.T. Watson, B. Grossman and R.T. Haftka, "A coarse grained variable-complexity approach to MDO for HSCT design," in *Parallel Processing for Scientific Computing*, D.H. Bailey, P.E. Bjørstad, J.R. Gilbert, M.V. Mascagni, R.S. Schreiber, H.D. Simon, V.J. Torczon and L.T. Watson (eds.), SIAM, Philadelphia, PA, 1995, pp. 96-101.

[14] ***em***™ and ***xgeom***™, Sonnet Software, Inc., 1020 Seventh North Street, Suite 210, Liverpool, NY 13088.

[15] A.A. Giunta, V. Balabanov, M. Kaufman, S. Burgee, B. Grossman, R.T. Haftka, W.H Mason and L.T. Watson, "Variable-complexity response surface design of an HSCT configuration," *Proceedings of the ICASE/LaRC Workshop on Multidisciplinary Design Optimization.* (Hampton, VA), 1995.

[16] M.G. Hutchison, X. Huang, W.H. Mason, R.T. Haftka and B. Grossman, "Variable-complexity aerodynamic-structural design of a high-speed civil transport wing," *4th AIAA/USAF/NASA/OAI Symp. Multidisciplinary Analysis and Optimization* (Cleveland, OH) 1992, paper 92-4695.

[17] D.M. Pozar, *Microwave Engineering*, Addison-Wesley, 1990.

[18] *OSA90/hope*™ and *Empipe*™, Optimization Systems Associates Inc., P.O. Box 8083, Dundas, Ontario, Canada L9H 5E7.

[19] J. Sacks, W.J. Welch, T.J. Mitchell and H.P. Wynn, "Design and analysis of computer experiments," *Statistical Science*, vol. 4, 1989, pp. 409-435.

[20] D.G. Swanson, Jr., "Using a microstrip bandpass filter to compare different circuit analysis techniques," *Int. J. Microwave and Millimeter-Wave Computer-Aided Engineering*, vol. 5, 1995, pp. 4-12.

[21] V.V. Toropov, "Simulation approach to structural optimization," *Structural Optimization*, vol. 1, 1989, pp. 37-46.

[22] V.V. Toropov, A.A. Filatov and A.A. Polynkin, "Multiparameter structural optimization using FEM and multipoint explicit approximations," *Structural Optimization*, vol. 6, 1993, pp. 7-14.

[23] S. Yesilyurt and A.T. Patera, "Surrogates for numerical simulations: optimization of eddy-promoter heat exchangers," *Computer Methods Appl. Mech. Eng.*, vol. 121, 1995, pp. 231-257.

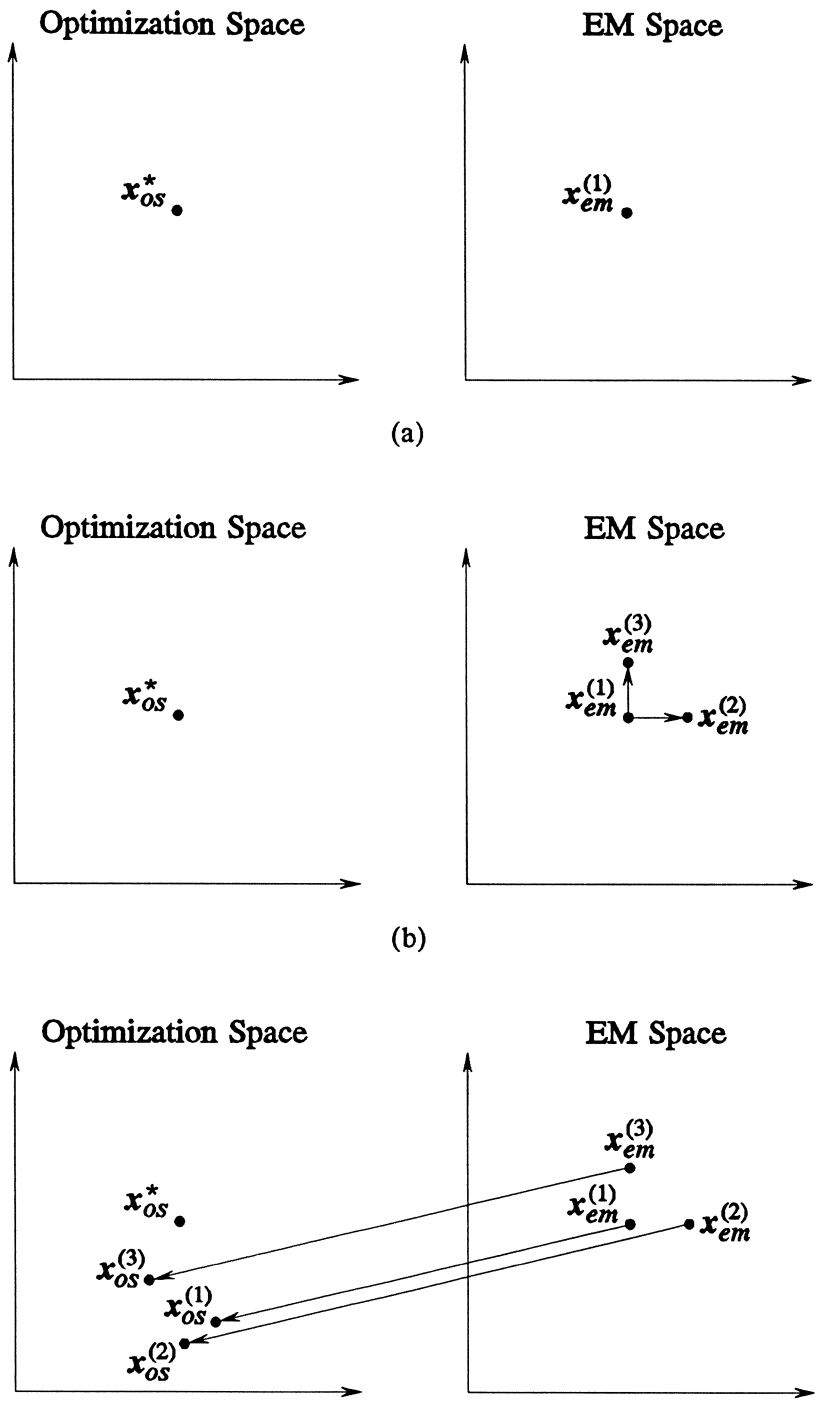

Fig. 1. Illustration of Space Mapping optimization: (a) set $x_{em}^{(1)} = x_{os}^*$, assuming x_{em} and x_{os} represent the same physical parameters, (b) generate additional base points around $x_{em}^{(1)}$, (c) perform X_{os}-space model parameter extraction according to (2.8).

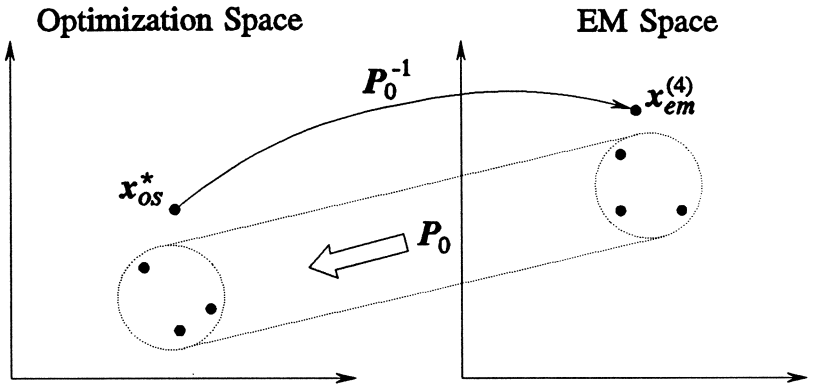

(d)

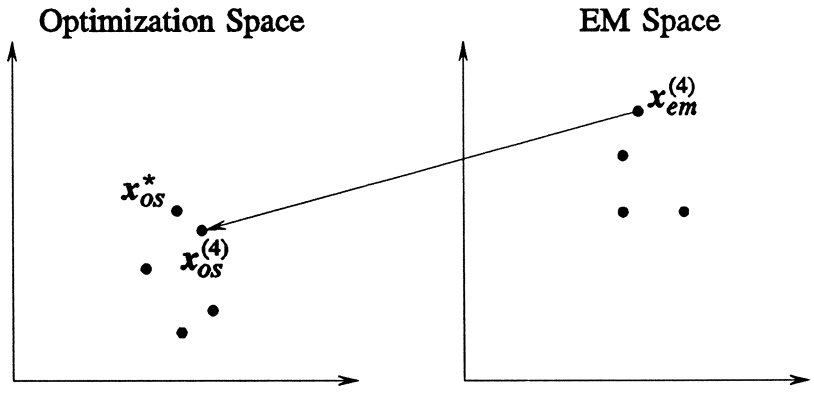

(e)

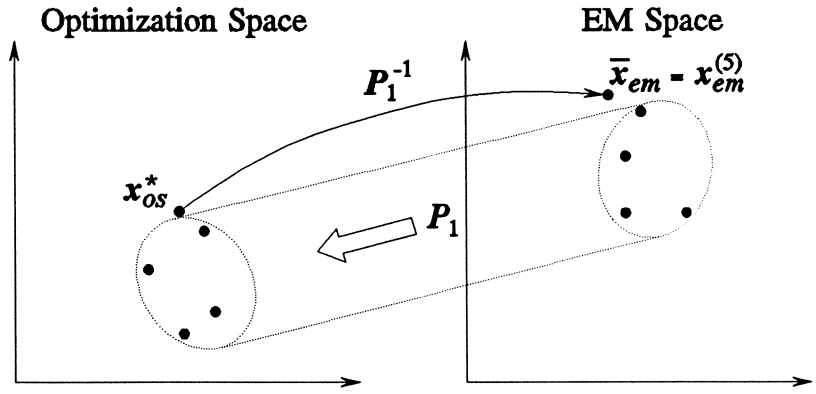

(f)

Fig. 1. Illustration of Space Mapping optimization (cont.): (d) use the inverse mapping to obtain $x_{em}^{(4)}$, (e) perform X_{os}-space model parameter extraction to obtain $x_{os}^{(4)}$, (f) apply the updated inverse mapping to obtain the SM solution $\bar{x}_{em} = x_{em}^{(5)}$, assuming $\| R_{os}(x_{os}^*) - R_{em}(x_{em}^{(5)}) \| \leq \epsilon$.

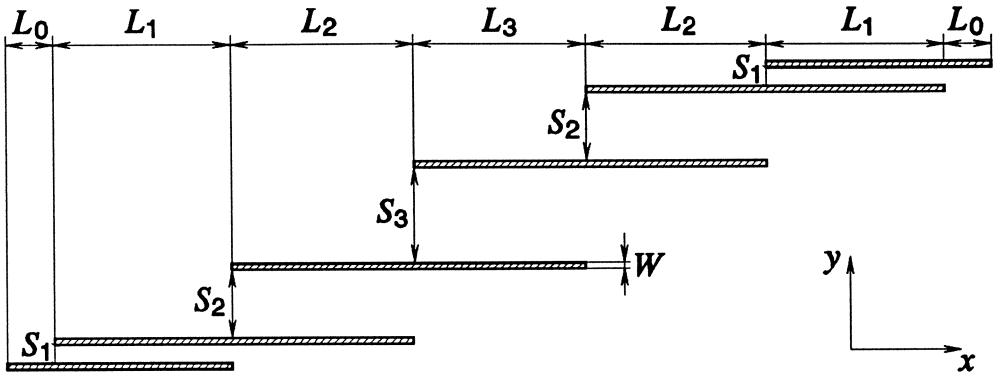

Fig. 2. The structure of the HTS filter.

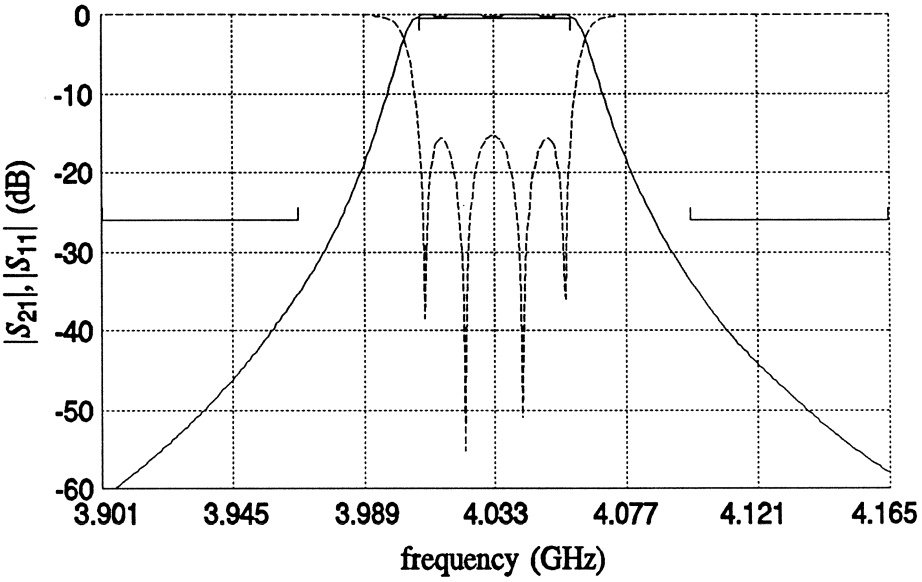

(a)

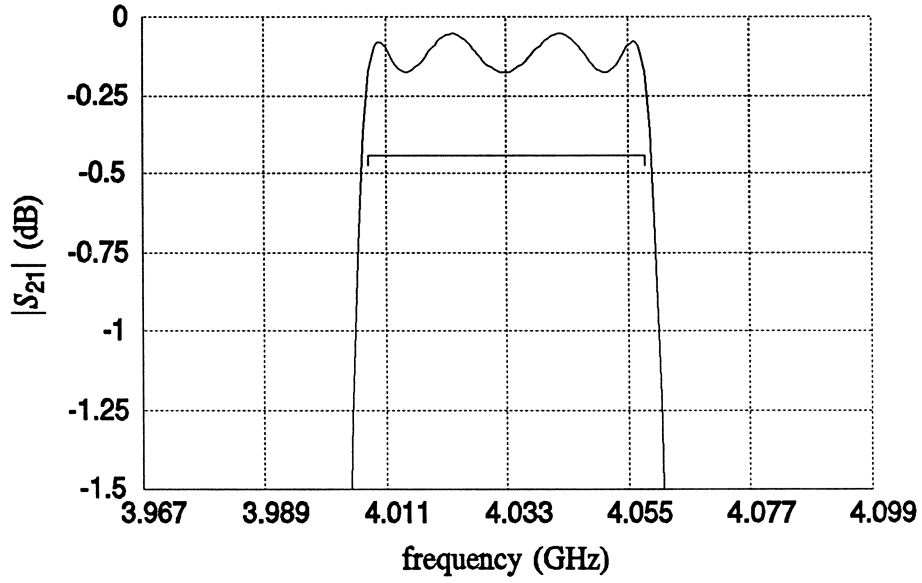

(b)

Fig. 3. The OSA90/hope empirical model responses after minimax optimization. (a) $|S_{21}|$ (——) and $|S_{11}|$ (---) for the overall frequency band and (b) the passband details of $|S_{21}|$. ⌊‾⌋ and ⌜‾⌝ denote the upper and lower design specifications, respectively.

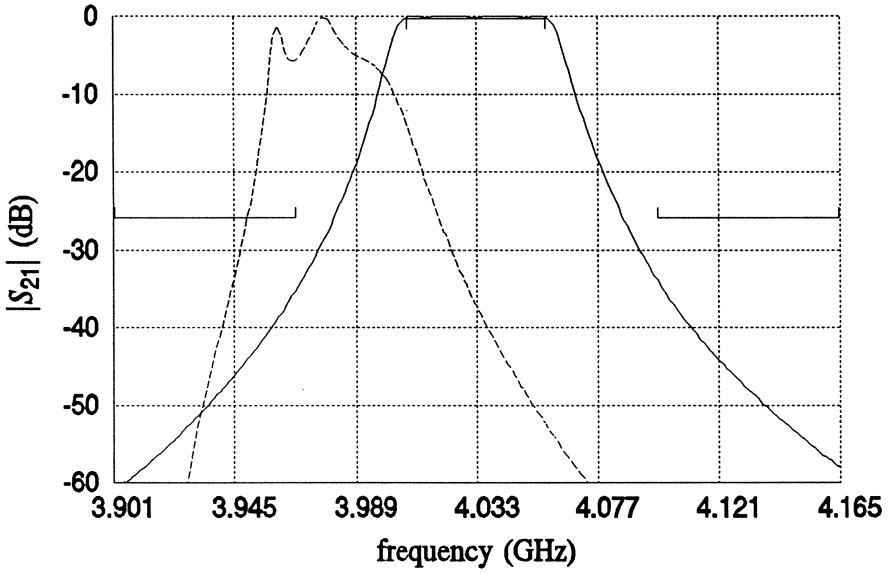

(a)

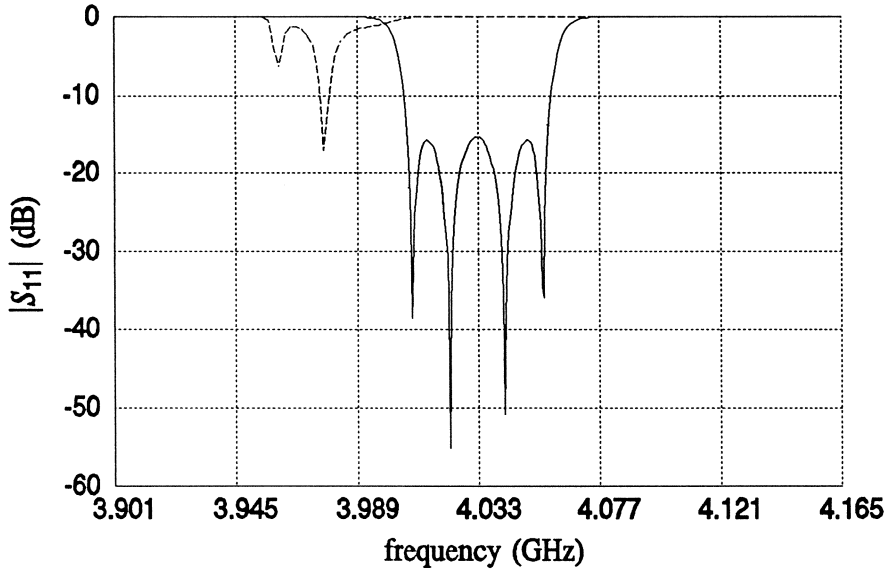

(b)

Fig. 4. A comparison of (a) $|S_{21}|$ and (b) $|S_{11}|$ between the empirical model (——) and ***em*** (---) at the empirical model minimax solution.

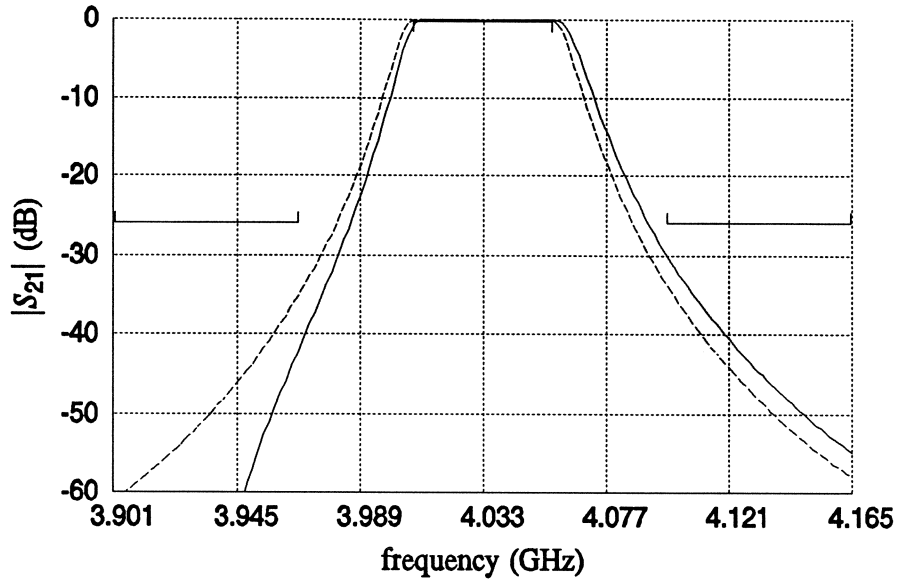

(a)

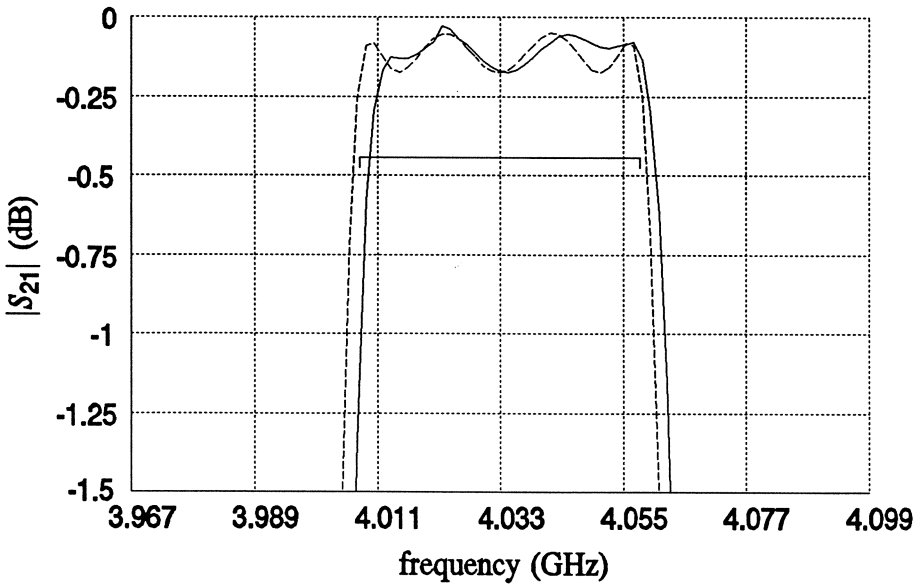

(b)

Fig. 5. The *em* simulated $|S_{21}|$ response of the HTS filter at the SM solution obtained using the aggressive SM approach (——). The OSA90/hope empirical model solution (---) is shown for comparison. Responses are shown for (a) the overall frequency band and (b) the passband in more detail.